Decreased expression of Drp1 and Fis1 mediates mitochondrial elongation in senescent cells and enhances resistance to oxidative stress through PINK1

Sören Mai[1], Michael Klinkenberg[2], Georg Auburger[2], Jürgen Bereiter-Hahn[1] and Marina Jendrach[1,2,*]

[1]Kinematic Cell Research Group, Institute for Cell Biology and Neuroscience, Center of Excellence Frankfurt: Macromolecular Complexes, Goethe University, Max-von-Laue-Str. 9, 60438 Frankfurt/Main, Germany
[2]Experimental Neurology, Department of Neurology, University Medical School, Heinrich-Hoffmann-Str. 7, Goethe University, 60590 Frankfurt/Main, Germany
*Author for correspondence (jendrach@bio.uni-frankfurt.de)

Accepted 3 January 2010
Journal of Cell Science 123, 917-926

doi:10.1242/jcs.059246

Summary

Mitochondria display different morphologies, depending on cell type and physiological situation. In many senescent cell types, an extensive elongation of mitochondria occurs, implying that the increase of mitochondrial length in senescence could have a functional role. To test this hypothesis, human endothelial cells (HUVECs) were aged in vitro. Young HUVECs had tubular mitochondria, whereas senescent cells were characterized by long interconnected mitochondria. The change in mitochondrial morphology was caused by downregulation of the expression of Fis1 and Drp1, two proteins regulating mitochondrial fission. Targeted photodamage of mitochondria induced the formation of reactive oxygen species (ROS), which triggered mitochondrial fragmentation and loss of membrane potential in young cells, whereas senescent cells proved to be resistant. Alterations of the Fis1 and Drp1 expression levels also influenced the expression of the putative serine-threonine kinase PINK1, which is associated with the PARK6 variant of Parkinson's disease. Downregulation of PINK1 or overexpression of a PINK1 mutant (G309D) increased the sensitivity against ROS in young cells. These results indicate that there is a Drp1- and Fis1-induced, and PINK1-mediated protection mechanism in senescent cells, which, when compromised, could contribute to the age-related progression of Parkinson's disease and arteriosclerosis.

Key words: Aging, Mitochondria, ROS, Drp1, Fis1, PINK1

Introduction

In many cells, from yeast to plants and mammals, mitochondria display significant dynamics by regularly undergoing fusion and fission (Bereiter-Hahn et al., 2008). Owing to mitochondrial dynamics, mtDNA and mitochondrial proteins can be continuously exchanged and distributed throughout the whole mitochondrial population (Ishihara et al., 2003; Busch et al., 2006; Ono et al., 2001). Fusion and fission are thus thought to act as a rescue mechanism for damaged mitochondria (Bossy-Wetzel et al., 2003; Chen et al., 2003; Kowald et al., 2005).

Fis1 and Drp1 are the main mitochondrial fission factors in mammalian cells (Smirnova et al., 1998; Frank et al., 2001; James et al., 2003; Stojanovski et al., 2004). The ubiquitously expressed kinase PINK1 also acts in *Drosophila melanogaster* as a mitochondrial fission factor (Poole et al., 2008), whereas its influence on mitochondrial morphology in mammalian cells remains controversial (Exner et al., 2007; Yang et al., 2008). Truncations of the PINK1 protein or mutations such as the G309D point mutation are linked with the autosomal recessive Parkinson's disease (PD) variant PARK6 (Valente et al., 2004), resulting in mitochondrial deficiencies characterized by complex I dysfunction, reduced membrane potential and increased oxidative stress (Exner et al., 2007; Gautier et al., 2008; Gispert et al., 2009).

The balance between mitochondrial fission and fusion depends on cell type and physiological situation; thus mitochondria can exhibit a tubular or a fragmented morphotype or can be assembled into networks. The equilibrium between fission and fusion is balanced towards fission before cytokinesis (Taguchi et al., 2007) or during stress (Lyamzaev et al., 2004; Perfettini et al., 2005; Jendrach et al., 2008). In many senescent postmitotic cell types, an extensive elongation of mitochondria occurs (Zottini et al., 2006; Yoon et al., 2006; Unterluggauer et al., 2007; Navratil et al., 2008), leading to the hypothesis that the elongation of mitochondria in old cells has a functional role. This hypothesis is supported by the fact that an increase of mitochondrial length by transient modulation of different mitochondrial fission and fusion factors confers resistance to apoptotic stimuli (Lee et al., 2004; Sugioka et al., 2004; Jahani-Asl et al., 2007). By contrast, fragmentation of mitochondria seems to contribute to neuronal pathology (Knott and Bossy-Wetzel, 2008).

Here, we investigated the significance of elongated and/or interconnected mitochondria in senescence by applying targeted photodamage to mitochondria of young and senescent cells. Mitochondria of senescent cells proved to be much more stress resistant, owing to Drp1- and Fis1-mediated mitochondrial elongation and increased PINK1 expression, thus indeed indicating a functional role for elongation of mitochondria in senescent cells.

Results

Age-induced changes of mitochondria in HUVECs

To determine the functional role of mitochondrial elongation in senescence, freshly isolated HUVECs were cultivated in vitro till they reached replicative senescence (supplementary material Fig. S1). Cell populations that had reached the stationary phase (doubling time more than 120 hours) and that contained more than 80% of

SA-β-galactosidase-positive cells (Fig. 1A), were classified as old and compared with young cells from the same isolation.

Mitochondria of young HUVECs exhibited mostly a tubular morphology (Fig. 1B). Mitochondrial length increased during aging, resulting in extended and interconnected mitochondria in senescent cells (Fig. 1B). The increase of mitochondrial length in age correlated with a significantly reduced expression of Fis1 and Drp1 in senescent cells as demonstrated by semi-quantitative RT-PCR and western blotting in different HUVEC isolations (Fig. 1C, supplementary material Fig. S1).

The mRNA expression levels of other known fission and fusion proteins (Opa1, Mfn1, Mfn2, SLP2 and MTP18) were analyzed by semi-quantitative RT-PCR and qPCR in up to six different HUVEC isolations. The transcript levels of Mfn1, Mfn2, Opa1 and MTP18 were not significantly altered and the transcript of SLP2, a protein causing hyperfusion in reaction to stress (Tondera et al., 2009), was strongly downregulated in senescent HUVEC (supplementary material Fig. S2), indicating that the elongation of mitochondria in aged HUVECs was mediated by decreased expression of Drp1 and Fis1.

Mitochondrial damage of young HUVECs after irradiation

The reaction of mitochondria in young and senescent cells toward stress was analyzed by application of mitochondrial-targeted photodamage. Mitochondria were stained with the mitochondria-specific photosensitizer MitotrackerRed CMX Ros (MTR) and irradiated with green light (0.3 J/cm^2) to evoke mitochondrial damage. MTR-stained, non-irradiated (control S) and non-stained, irradiated cells (control I) served as controls. The chosen irradiation regime induced transient mitochondrial damage but not premature aging or apoptosis, because no release of cytochrome c or an increase of apoptotic nuclei was observed in young and senescent cells after irradiation (supplementary material Figs S3-S6).

Starting from 1 hour after irradiation of young MTR-stained HUVECs, an increasing percentage of cells contained tubular mitochondria with swollen regions (intermediate morphotype) or small rounded mitochondria (fragmented morphotype) (Fig. 2A). By contrast, almost all control cells displayed the typical tubular mitochondrial morphology of young HUVECs. Quantification of the different mitochondrial morphologies revealed the highest amount of cells with fragmented mitochondria 8 hours after irradiation. After 24 hours, mitochondrial morphology started to return to its former tubular state and recovery was completed within 72 hours (Fig. 2A).

Eight hours after irradiation, which was the time point with the highest percentage of cells with fragmented mitochondria, HUVECs were stained with the dye DASPMI. A strong DASPMI fluorescence indicates a high membrane potential (Ramadass and Bereiter-Hahn, 2008), as exhibited by mitochondria of both controls (Fig. 2B). Irradiated cells however, displayed in addition to mitochondrial fragmentation, a significant loss of their membrane potential, discernible by the release of DASPMI to the cytoplasm. Taken together, young cells were sensitive to mitochondrial-targeted photodamage, which evoked a massive mitochondrial fragmentation and loss of membrane potential.

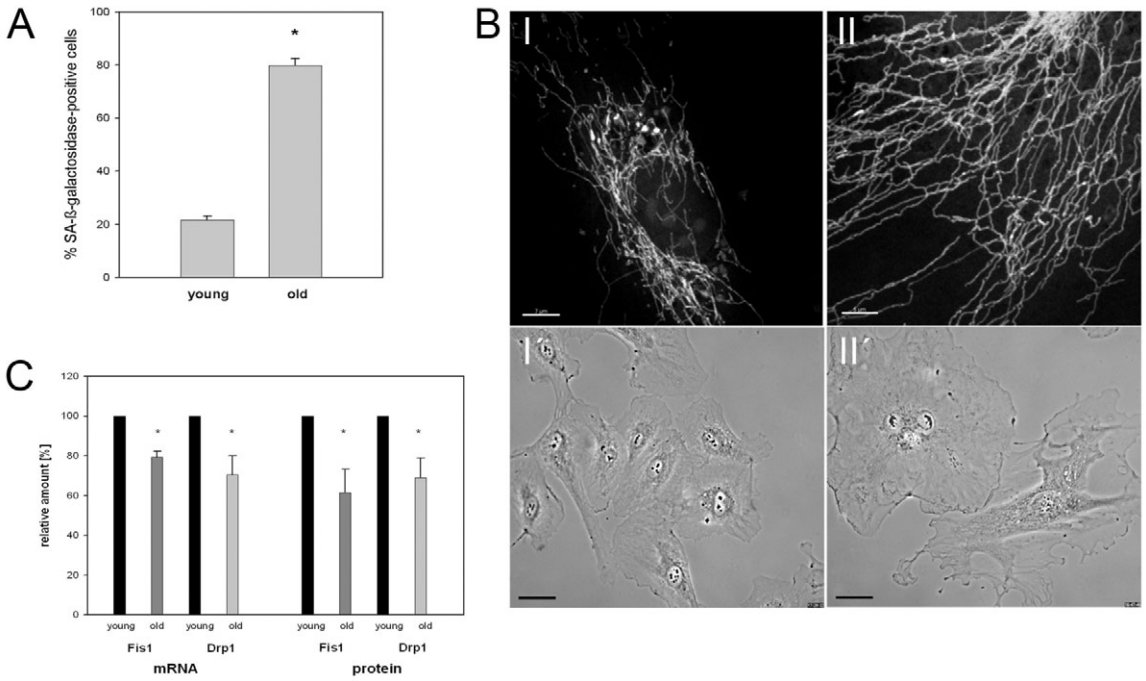

Fig. 1. Elongation of mitochondria in senescent HUVECs. (**A**) Young, proliferating and old postmitotic HUVECs stained for the senescence marker SA-β-galactosidase. When more than 80% of the HUVECs expressed SA-β-galactosidase, cells were defined as old and postmitotic. At least 200 cells were counted per experiment; *n*=3. (**B**) Mitochondria of young cells stained with MTR exhibit tubular mitochondria (I); with age, mitochondria become more elongated and branched (II). Also the size of old cells increases, depicted in the phase-contrast images of young (I′) and old (II′) cells. Scale bars: 50 µm. (**C**) Relative mRNA levels and protein levels of Fis1 and Drp1 in young and old HUVECs from different isolations were determined by semiquantitative RT-PCR and western blotting, respectively. The fission factor levels were normalized to β-actin mRNA expression. The expression ratios of young cells were set as 100%. A significant reduction of the mRNA (Fis1 79.2%; Drp1 70.4%) and protein expression of Fis1 (61.4%) and Drp1 (69.1%) occurred in old HUVECs; mRNA, **P*<0.005 (Fis1), *n*=5; **P*<0.05 (Drp1), *n*=6; protein, **P*<0.05 (Fis1), *n*=3; **P*<0.05 (Drp1), *n*=3.

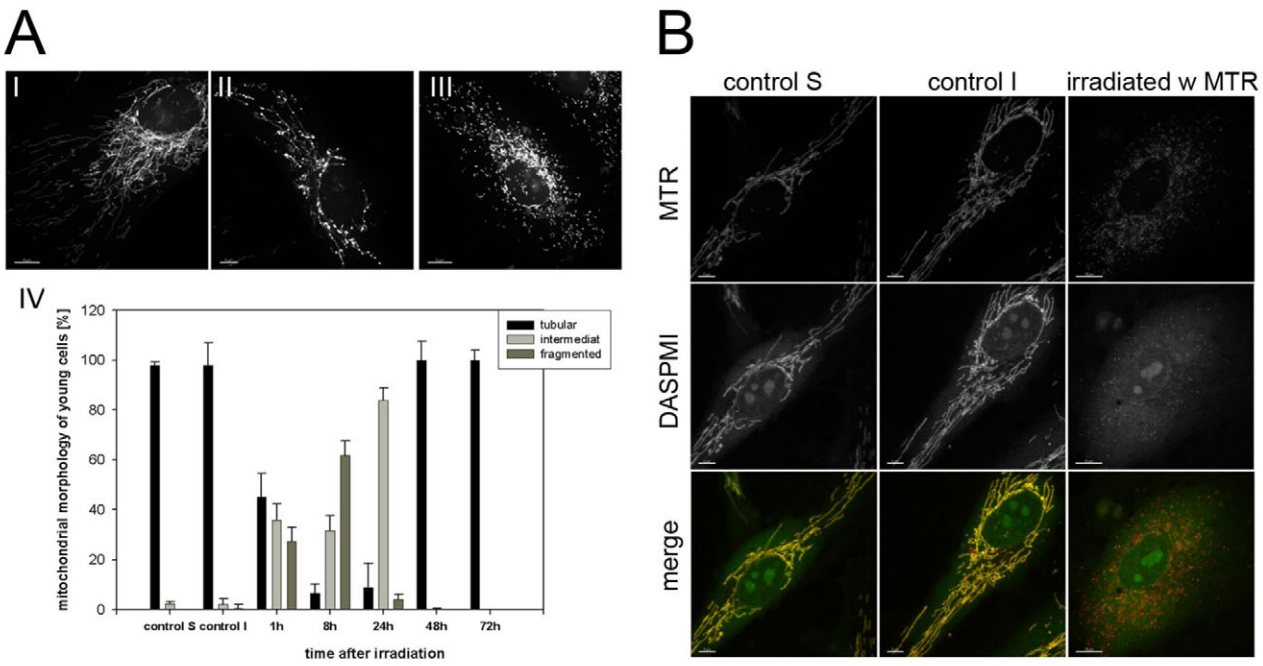

Fig. 2. Irradiation of young HUVECs induces mitochondrial fragmentation. (**A**) Cells were either stained with MTR and not irradiated (control S), or irradiated without MTR staining (control I), or MTR stained and irradiated (0.3 J/cm^2). Mitochondrial morphology was divided into three morphotypes: tubular (I), intermediate (swollen parts within tubular mitochondria) (II) and fragmented (small rounded mitochondria) (III). (IV) Quantification of the mitochondrial morphology (mean ± s.e.m.) in stained and irradiated cells shows the greatest number of cells with fragmented mitochondria 8 hours after irradiation. For both controls, only the average over the whole time is represented; at least 100 cells/sample; n=6. (**B**) 8 hours after irradiation, the mitochondrial membrane potential was analyzed with the dye DASPMI. Both controls show strong DASPMI fluorescence in the mitochondria, indicating a high membrane potential. In MTR-stained and irradiated cells, fragmented mitochondria and cytoplasmic DASPMI fluorescence become evident, implying loss of membrane potential.

Resistance of mitochondria in senescent HUVECs against targeted irradiation

By contrast, irradiation of senescent MTR-stained HUVECs evoked mitochondrial fragmentation in at most 5% of the cells (Fig. 3A). When the irradiation time was extended to 30 minutes, mitochondrial fragmentation also occurred in old cells, indicating that the mitochondrial fission machinery itself was functional (data not shown).

The minimal fragmentation of mitochondria of old HUVECs could be caused by reduced uptake of MTR owing to the lower membrane potential of senescent HUVECs. Therefore, old HUVECs were stained with 40 nM MTR, resulting in the same MTR fluorescence intensity as staining of young cells with 25 nM MTR (data not shown). Thus, young cells were stained with 25 nM MTR and senescent HUVECs with 40 nM MTR, and the mitochondrial morphology was analyzed 8 hours after irradiation. Despite the adjustment of the MTR concentration, the number of senescent cells with fragmented mitochondria only increased by 6%, indicating a different mechanism behind the stress resistance of old HUVECs (Fig. 3B).

Although the mitochondrial membrane potential in old cells was in general lower than in young ones, it did not differ between irradiated MTR-stained cells and control cells 8 hours after irradiation, as shown by the equal DASPMI staining of all three samples (Fig. 3C). Thus, these results demonstrate that elongated and interconnected mitochondria of senescent cells had a much higher threshold for irradiation-induced mitochondrial damage than the single mitochondria of young cells did.

Irradiation triggers ROS production that induces mitochondrial fragmentation

To understand the mechanism that protects mitochondria of senescent cells, we first investigated the signal that induced the mitochondrial damage after irradiation. As photodamage can increase the production of reactive oxygen species (ROS) (Collins et al., 2002; Neuspiel et al., 2005), the cellular ROS content was determined immediately after irradiation. Irradiated cells demonstrated a significant ROS increase compared with non-irradiated cells, confirming that irradiation of MTR-stained mitochondria induced oxidative stress (Fig. 4A). The functional significance of ROS formation was supported by the increased amount of carbonylated proteins that was detected after irradiation by oxyblotting (Fig. 4B). To prove that ROS can directly induce mitochondrial fragmentation, young cells were preincubated with the antioxidant N-acetylcysteine (NAC) and irradiated. Addition of NAC protected cells significantly against mitochondrial fragmentation (Fig. 4C), implying that ROS acts either as initiator or as messenger in a signaling process, which results in mitochondrial fragmentation.

Mitochondrial elongation and PINK1 upregulation protect old cells against oxidative stress

A tilt of the balance of mitochondrial dynamics towards mitochondrial fusion renders different cell types more stress resistant (Lee et al., 2004; Sugioka et al., 2004; Jahani-Asl et al., 2007). Thus, we hypothesized that the enhanced protection of senescent cells against ROS-induced damage could be provided through an

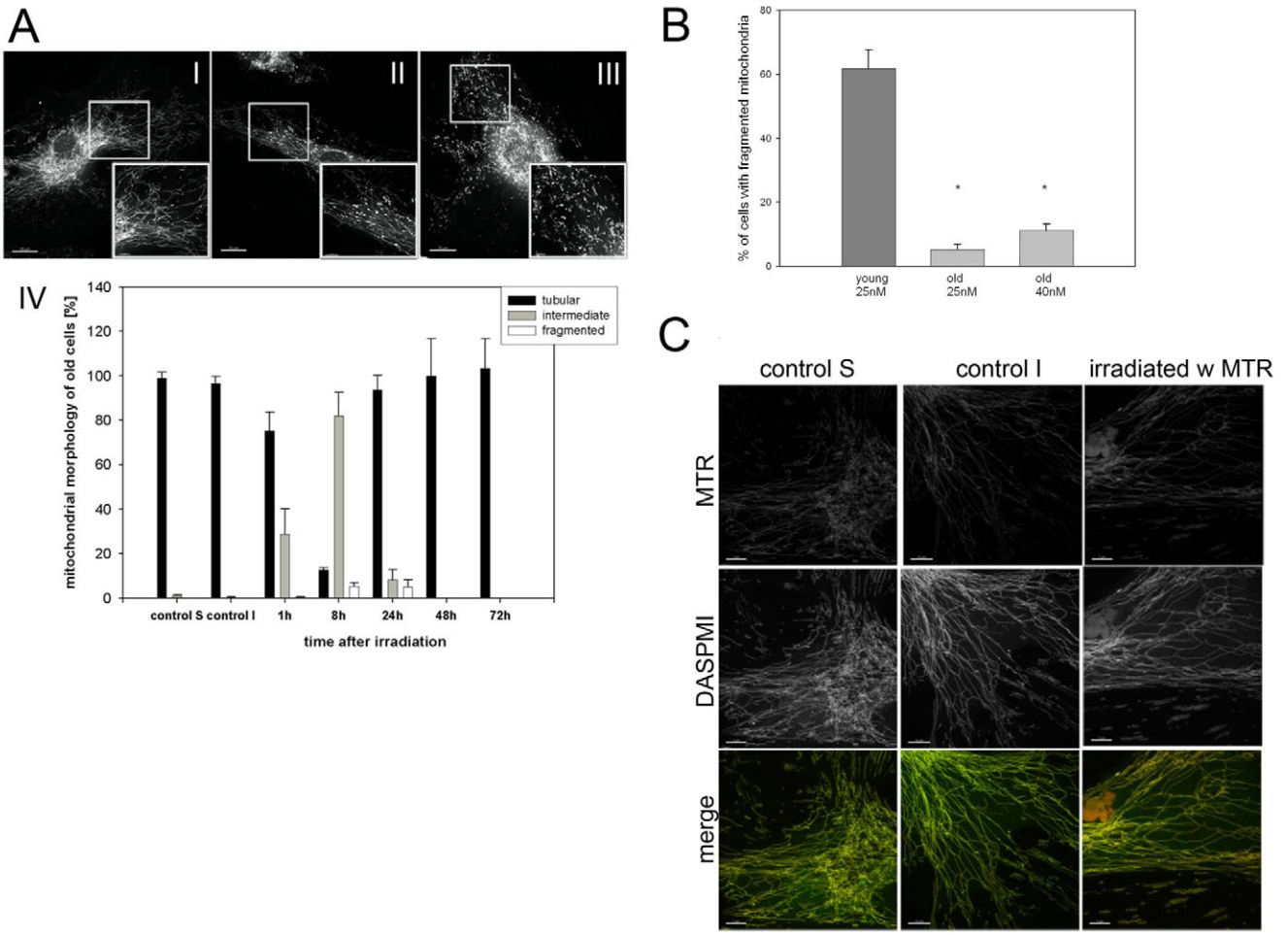

Fig. 3. Senescent HUVECs exhibit resistance against irradiation-induced damage. (**A**) Senescent cells were either not stained and irradiated (control I), stained with 25 nM MTR and not irradiated (control S), or MTR-stained and irradiated. The morphology of the mitochondria was classified into three categories: tubular and/or network (I), intermediate (II) and fragmented (III). Only a small number of old cells exhibited fragmented mitochondria after staining and irradiation (IV). For both controls, only the average over the whole time is represented; at least 100 cells/sample; n=3. (**B**) Increase in MTR staining concentration for old cells from 25 nM to 40 nM resulted in an equal relative mitochondrial MTR fluorescence in young and old HUVECs, but increased only slightly the percentage of cells with fragmented mitochondria 8 hours after irradiation; n=4, *P<0.05. (**C**) Senescent cells were stained with 40 nM MTR and irradiated, controls were either stained with 40 nM MTR and not irradiated (control S) or irradiated without previous staining (control I). After 8 hours, both controls and irradiated cells exhibited a comparable DASPMI fluorescence, indicating that the membrane potential remained intact.

intramitochondrial replacement of damaged mitochondrial components. To assess this hypothesis, senescent HUVECs transfected with photoactivatable GFP targeted to the mitochondrial matrix (mt-PaGFP) were used. After photoactivation of a distinct region of interest (ROI) in the mitochondria, extensive spreading of the GFP fluorescence was observed throughout the mitochondrial network within seconds (Fig. 5A). This experiment clearly shows that fast intramitochondrial distribution of ROS and/or damaged mitochondrial components can occur, supporting the hypothesis that the ROS resistance of cells with elongated mitochondria is related to the mitochondrial architecture.

To determine whether additional mechanisms protect senescent HUVECs from ROS-induced fragmentation, a transcriptome analysis from young and old HUVECs of three different isolations was performed. mRNA expression profiling revealed an increase of *PINK1* mRNA in senescent cells, which was confirmed by qPCR (Fig. 5B). PINK1 protein levels could not be determined, because no commercially available antibody detects endogenous PINK1 (Zhou et al., 2008). To determine whether PINK1 has a functional role in the stress resistance of endothelial cells, young HUVECs were transfected with either a siRNA against *PINK1* or a scrambled siRNA. In cells transfected with *PINK1* siRNA, levels of *PINK1* mRNA were strongly reduced 48 hours after transfection (Fig. 5C). Interestingly, under normal conditions, downregulation of PINK1 protein had no effect on mitochondrial morphology (Fig. 5D), indicating that PINK1 itself does not act as fission or fusion factor in HUVECs. However, irradiation of cells treated with *PINK1* siRNA yielded a significantly higher amount of cells containing fragmented mitochondria (Fig. 5E). Also, overexpression of a kinase-deficient *PINK1* mutant (G309D) resulted in a significant increase of cells with fragmented mitochondria after irradiation (Fig. 5E), implying that senescent cells are also protected against oxidative damage by their elevated PINK1 levels.

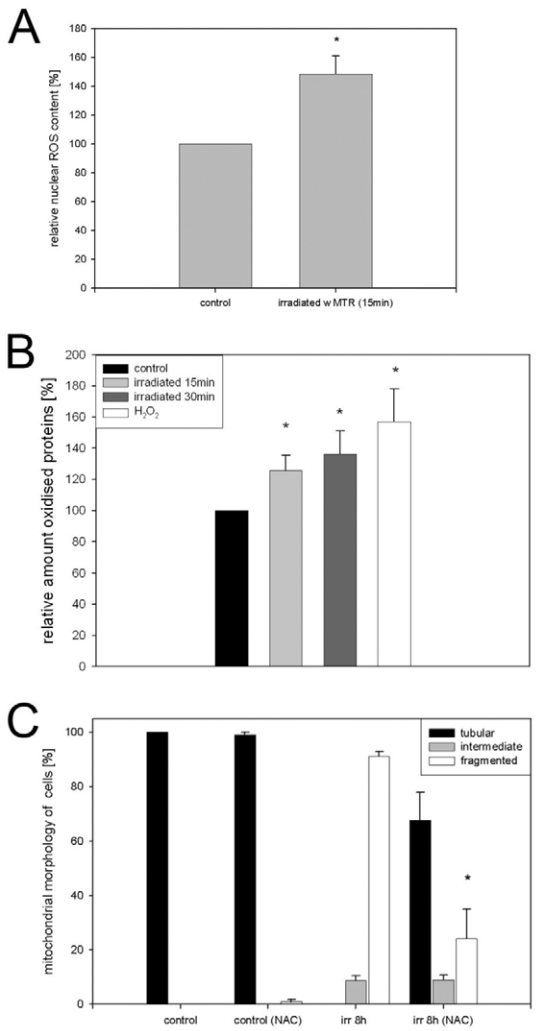

Fig. 4. Irradiation-induced ROS increase triggers mitochondrial fragmentation. (**A**) Young HUVECs were stained with MTR and, after 30 minutes, were stained with the ROS-sensitive dye DHE and irradiated. The relative ethidium fluorescence was determined immediately after cells were irradiated; the relative fluorescence intensity of non-irradiated cells was set to 100%. Irradiation of MTR-stained cells induced a significant ROS increase; n=7; at least eight fields of view per experiment. *P<0.005. (**B**) The oxidative modification of cellular proteins after 15 and 30 minutes of irradiation was determined by oxyblotting; addition of 9.8 mM hydrogen peroxide for 10 minutes served as a positive control. The relative amount of oxidized proteins of control cells was set to 100%. Increasing irradiation times result in an elevated amount of carbonylated proteins; n=11, *P<0.05 for all three conditions. (**C**) Young cells were stained with MTR and then preincubated for 24 hours with the ROS scavenger NAC. Mitochondrial morphology was determined 8 hours after irradiation. NAC protected irradiated cells effectively from fragmentation, indicating that ROS do trigger mitochondrial fragmentation after irradiation. The irradiation time was prolonged for this set of experiments to 2-17 minutes; n=9; at least 100 cells/experiment were analyzed, *P<0.00005.

This conclusion correlates with data which show that overexpression of PINK1 can protect cells against different stressors (Petit et al., 2005; Pridgeon et al., 2007; Haque et al., 2008). To mimic elevated PINK1 levels in young HUVECs, cells were transfected with two different PINK1-GFP plasmids, respectively; however, transfection of both constructs caused massive apoptosis after 24 hours. Therefore, DNA concentration of PINK1-GFP2 was reduced by half, and a construct with the weaker SV40 promoter instead of the CMV promoter in front of PINK-GFP was created. Also, these two approaches resulted in a loss of strongly transfected HUVECs that were discernable by microscopy 48 hours after transfection. The surviving cells exhibited either already fragmented mitochondria, thus rendering them useless for the irradiation experiment, or no GFP fluorescence at all (data not shown). Taken together, these data demonstrate that PINK1 levels must be tightly balanced and regulated.

Drp1 and Fis1 levels regulate PINK1 expression

In senescent HUVECs, a reduced expression of Drp1 and Fis1 correlated with increased *PINK1* mRNA levels (Fig. 1C, Fig. 5B), indicating a putative relationship between Drp1, Fis1 and PINK1. To reproduce this feature, young HUVECs were treated with a siRNA directed against *FIS1*. In a second approach, cells were transfected with a siRNA directed against *DRP1*, or with both siRNAs together. A time course showed that 72 hours after transfection of the Fis1 siRNA, endogenous Fis1 protein levels were reduced by 81% compared with levels in cells transfected with scrambled siRNA (Fig. 6A,B). Addition of *DRP1* siRNA resulted in a reduction of 71% after 72 hours, and both siRNAs together also caused a signification downregulation of endogenous Fis1 and Drp1 levels (Fig. 6A,B). qPCR revealed a significant upregulation of endogenous *PINK1* mRNA levels 72 hours after downregulation of Fis1 or Drp1 (Fig. 6C). In correlation with the results on old HUVECs, an additive effect on the *PINK1* mRNA upregulation was observed 72 hours after the transient knockdown of both fission factors (Fig. 6C).

To achieve the opposite effect, GFP-Fis1, GFP-Drp1 and a dominant-negative mutant of Drp1, Drp1 K38A, were overexpressed in young HUVECs. At 48 hours after transfection, *PINK1* mRNA levels were accordingly strongly reduced in cells transfected with GFP-Fis1 and GFP-Drp1 (Fig. 6D). This effect was also apparent in cells transfected with Drp1 K38A, but not as strong as in HUVECs transfected with the functional fission factors (Fig. 6D).

Downregulation of PINK1 by siRNA did not alter the expression of Drp1 or Fis1 (data not shown). Taken together, these data imply that Drp1 and Fis1 act upstream of PINK1 and regulate its expression (summarized in Fig. 7).

Discussion

Here, we investigated a putative functional role for mitochondrial elongation in age. HUVECs were chosen for this study because this cell type has an important role for in vivo aging by undergoing a prolonged senescent phase, and senescent endothelial cells probably contribute to the development of arteriosclerosis (Erusalimsky and Kurz, 2006). In senescent HUVECs, mitochondria were elongated and interconnected. The mitochondrial fission factors Drp1 and Fis1 were significantly reduced in aged cells, whereas Mfn1, Mfn2, Opa and MTP18 were not significantly altered. Interestingly, *MFN1* and *MTP18* mRNA levels exhibited much higher variations than the other analyzed fission and fusion factor mRNAs. Since a high variability of *MTP18* mRNA expression was also observed after hydrogen peroxide stimulation of HUVECs (Jendrach et al., 2008), *MTP18* mRNA levels could represent a marker for the variability between different HUVEC isolations.

In young or immortalized cells, exchange of mitochondrial components and also damaged molecules is achieved by frequent fusion and fission of mitochondria (Nakada et al., 2001; Ishihara

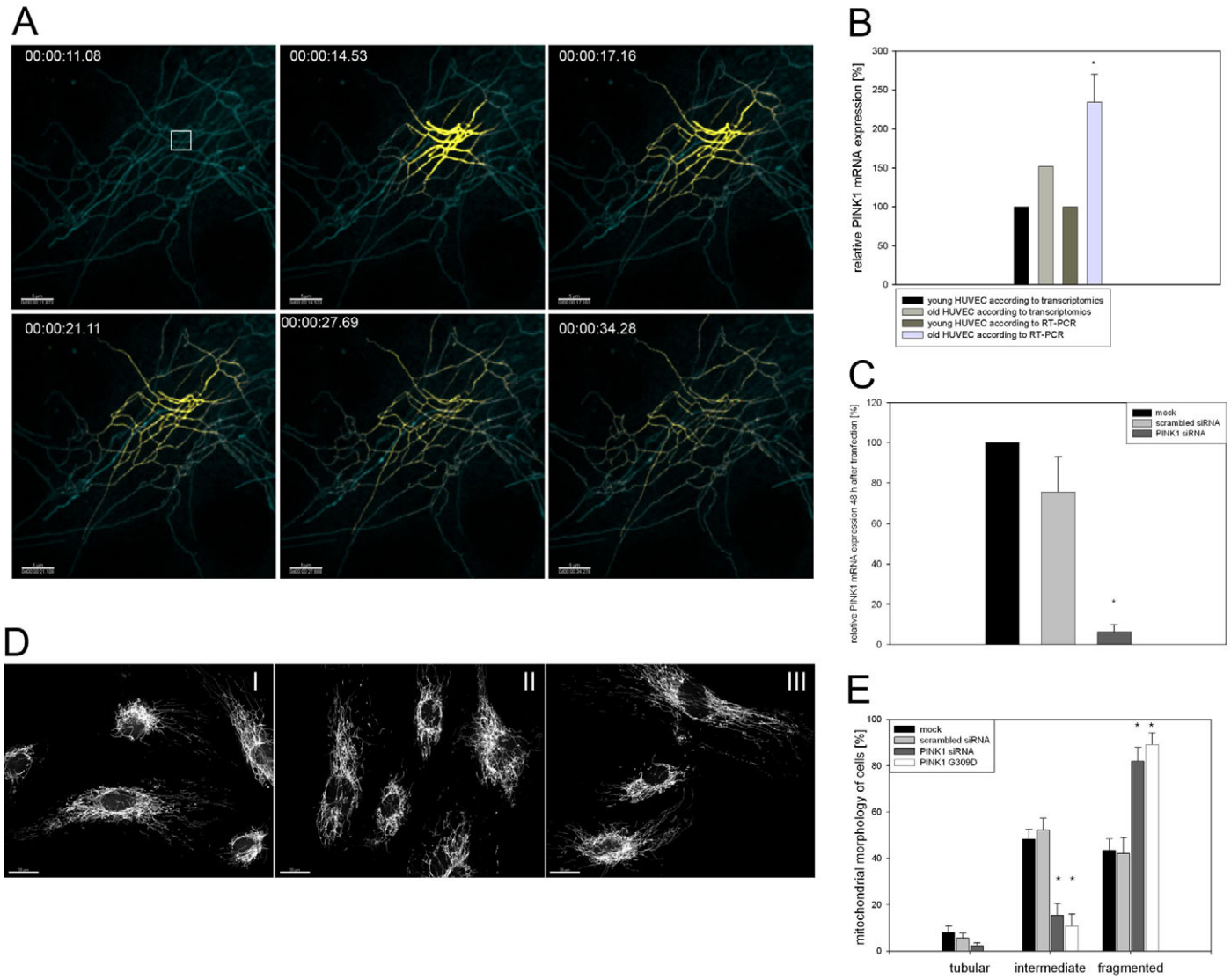

Fig. 5. Drp1- and Fis1-induced upregulation of PINK1 protects against oxidative stress. (**A**) A small ROI (square) was activated by UV radiation in mitochondria of senescent HUVECs that expressed stable transfected mitochondrial matrix-targeted photoactivatable GFP. The fast diffusion of the photoactivated GFP throughout the mitochondrial network demonstrates its coherence and interconnectivity; Scale bars: 5 µm. (**B**) The relative *PINK1* mRNA level in young and old HUVECs from three different isolations was determined by transcriptome profiling and qRT-PCR. The *PINK1* mRNA expression of young cells was set for both methods to 100%. *PINK1* mRNA was significantly increased in senescent cells; **P*<0.05; *n*=3. (**C**) Young HUVECs were transiently transfected with PINK1 siRNA or scrambled siRNA. *PINK1* mRNA levels were determined 48 hours after transfection by qPCR and the amount of *PINK1* transcript of mock-transfected cells was set to 100%. Cells transfected with *PINK1* siRNA exhibited an almost complete reduction of *PINK1* mRNA; *n*=3; **P*<0.05. (**D**) Mitochondrial morphology of non-irradiated young cells, which were either mock-transfected (I) or transfected with scrambled siRNA (II) or *PINK1* siRNA (III), analyzed 48 hours after transfection. Cells retained their tubular morphology, indicating that no morphology-altering effect occurred after PINK1 downregulation. (**E**) Young HUVECs transfected with *PINK1* siRNA, scrambled siRNA or a mutant of PINK1 (G309D) were irradiated. When the mitochondrial morphology was determined 8 hours after irradiation, a strong increase of cells with fragmented mitochondria was observed in cells transfected with *PINK1* siRNA and *PINK1* G309D mutant compared with control cells, implying that loss of functional PINK1 sensitized cells to oxidative stress. The irradiation time was reduced for this set of experiments to 1-14 minutes; *n*=8; **P*<0.05.

et al., 2003; Busch et al., 2006); both processes require different GTPases for the actual fission and fusion processes, and also ATP- and GTP-driven motor proteins. In senescent cells, however, mitochondrial dynamics are strongly reduced (Jendrach et al., 2005). Elongation of mitochondria allows for a rapid distribution of molecules in the mitochondrial matrix, as demonstrated by the inverse FRAP experiment in old HUVECs. Hence, the formation of long and interconnected mitochondria in senescent cells would diminish the need for the energy-consuming processes of mitochondrial dynamics, while still allowing fast distribution and exchange of molecules.

This hypothesis is enforced by data which demonstrate that elongation of mitochondria rendered cells more resistant against apoptotic stimuli (Lee et al., 2004; Sugioka et al., 2004; Jahani-Asl et al., 2007), whereas an imbalance towards mitochondrial fission is possibly connected to neuronal damage (Knott and Bossy-Wetzel,

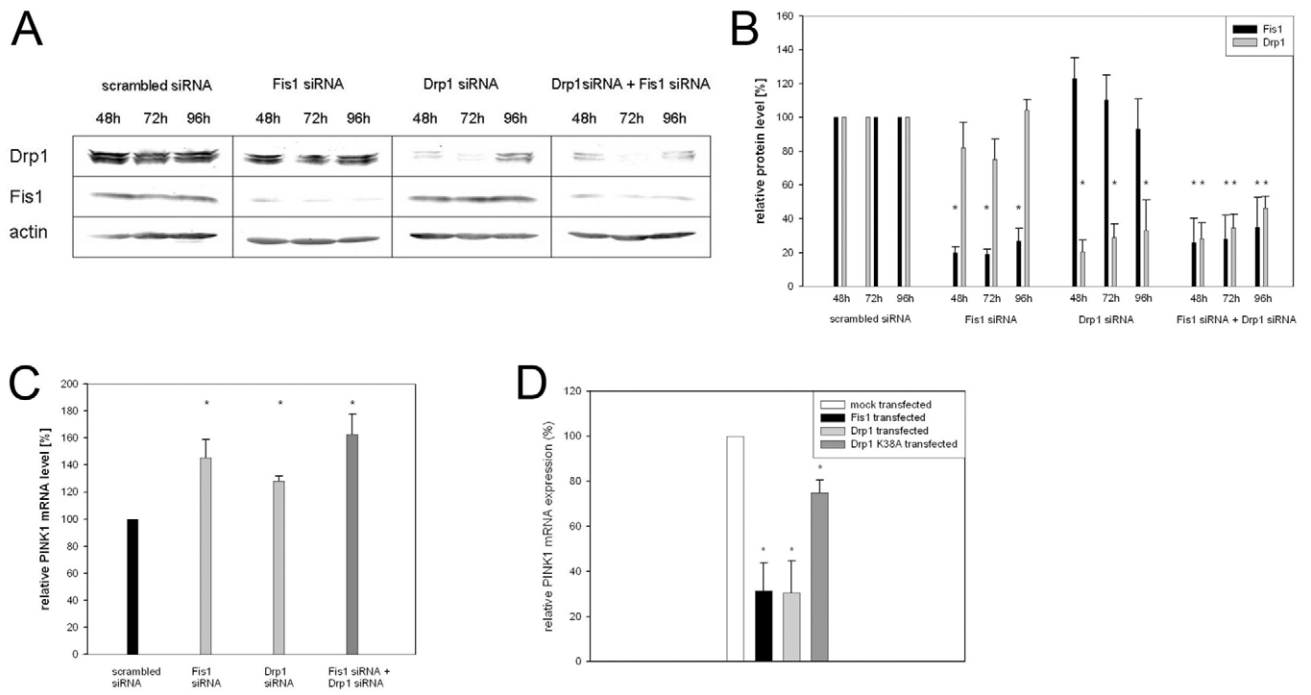

Fig. 6. Drp1 and Fis1 levels regulate *PINK1* mRNA expression. (**A**) Young HUVECs were transiently transfected with *FIS1* siRNA, *DRP1* siRNA, both *FIS1* siRNA and *DRP1* siRNA, or scrambled siRNA. The protein levels of Fis1, Drp and actin were determined by western blotting 48, 72 and 96 hours after transfection. There was a strong reduction in levels of Fis1 and Drp1 proteins after transfection of the respective siRNA. (**B**) The quantification of the western blots in A revealed after normalization that the relative Fis1 protein expression was downregulated by 81% and the relative Drp1 protein level reduced by 71% compared with levels in cells transfected with the scrambled siRNA 72 hours after transfection. The transient knockdown of both proteins together resulted in 28% remaining Fis1 protein and 35% remaining Drp1 protein. n=3; Fis1 knockdown, *P<0.0005 (alone) and *P<0.01 (with Drp1); Drp1 knockdown, *P<0.001 (alone) and *P<0.005 (with Fis1). (**C**) Young HUVECs were transfected with siRNA against *FIS1*, siRNA against *DRP1*, and siRNAs against *FIS1* and *DRP1* for 72 hours. Afterwards, the amount of *PINK1* mRNA was determined by qPCR. The mRNA expression level of scrambled-siRNA-transfected cells was set at 100%. Reduction of both fission factors alone or in combination resulted in increased *PINK1* mRNA expression; n=3; siRNA *FIS1*: P<0.05; siRNA *DRP1*: P<0.005; siRNA *FIS1* and *DRP1*: P<0.05. (**D**) Young HUVECs were transfected with GFP-Fis1, GFP-Drp1 or GFP-Drp1 K38A, and 48 hours after transfection, the *PINK1* mRNA levels were quantified by qPCR. The transcript of mock-transfected cells was set at 100%. A significant reduction of *PINK1* mRNA was observed after transfection of all three constructs; GFP-Fis1, n=3, *P<0.01; GFP-Drp1, n=3, *P<0.01; GFP-Drp1 K38A, n=3, *P<0.05.

2008). Most probably for the same reason, mitochondrial hyperfusion takes place in mouse embryonic fibroblasts after application of stress (Tondera et al., 2009). This process is mediated by SLP2, a protein that is strongly downregulated in senescent cells, implying that mitochondrial hyperfusion acts as a prosurvival mechanism against stress in only proliferating cells, because this feature would become obsolete in postmitotic cells where mitochondria are permanently elongated.

Downregulation of *PINK1* expression by siRNA or overexpression of the PD-related G309D mutant without an active kinase domain did not alter the mitochondrial morphology. Similar observations were made in cells derived from *PINK1*-knockout mice (Gautier et al., 2008; Gispert et al., 2009), whereas other groups detected increased fission after loss of active PINK1 (Exner et al., 2007; Lutz et al., 2009; Sandebring et al., 2009). However, loss of active PINK1 rendered young HUVECs more sensitive against irradiation-induced stress, correlating with data that demonstrate an increased sensitivity to Drp1-induced mitochondrial fragmentation after knockdown of PINK1 (Lutz et al., 2009; Sandebring et al., 2009). Thus, the effects of PINK1 knockdown on mitochondrial morphology are probably influenced by the stress to which cells are subjected. This is further supported by our observation that overexpression of different *PINK1* constructs caused apoptosis in HUVECs. Surviving cells exhibited fragmented mitochondria, indicating that at least in HUVECs, mitochondrial fragmentation after PINK1 overexpression is most probably a secondary effect and stress related. Furthermore, a tight control of PINK1 expression levels seems to be necessary to ensure cellular and mitochondrial fitness.

We detected another interesting link between PINK1 and mitochondrial fission: age-induced downregulation of Drp1 and Fis1 in old cells mediated a moderate increase in *PINK1* mRNA expression. Further experiments with Drp1 and Fis1 in young HUVECs demonstrated that both fission factors were able to regulate the PINK1 expression separately. By contrast, overexpression of Drp1, Drp1 K38A and Fis1 reduced *PINK1* mRNA levels. Although Drp1 and Fis1 exhibited quite a strong effect, overexpression of the mutant Drp1 K38A was less efficient in regulating *PINK1* mRNA. This could be either because of varying expression levels or because the active fission protein is more efficient in the regulation of PINK1. Further experiments should elucidate the molecular-signaling pathway controlling Fis1- and Drp1-mediated *PINK1* mRNA expression. In summary, these data demonstrate clearly that PINK1 does not act as fission or fusion factor in HUVECs, but is rather regulated by the active fission factors Drp1 and Fis1.

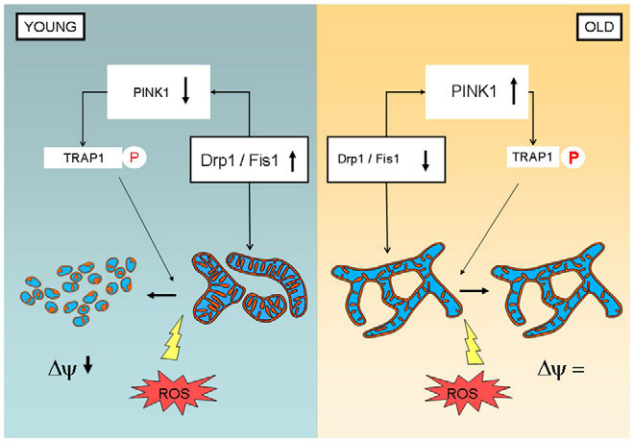

Fig. 7. Proposed protection mechanisms against oxidative stress in old cells. Addition of oxidative stress induces fragmentation and loss of mitochondrial membrane potential in young cells, but not in old cells. The protection of old cells is mediated by the reduced expression of the fission factors Drp1 and Fis1. This causes an elongation of mitochondria resulting in long interconnected mitochondria as well as a moderate elevation of PINK1 levels. The altered mitochondrial architecture, as well as an increased PINK1-mediated phosphorylation of TRAP1, protect mitochondria of senescent cells against ROS-induced fragmentation.

The Drp1- and Fis1-mediated upregulation of *PINK1* expression in senescent HUVECs seems to present an additional protection mechanism against oxidative damage in mitochondria. In PC12 cells, overexpression of PINK1 protein conferred resistance against oxidative stress-induced apoptosis by phosphorylation of the mitochondrial chaperone TRAP1 (Pridgeon et al., 2007) and TRAP1 has been shown to reduce ROS directly in mitochondria (Hua et al., 2007). Mitochondria in young HUVECs with a moderate PINK1 overexpression were less inclined to fragment after irradiation, whereas transfection of *PINK1* siRNA or overexpression of the G309D mutant mediated a strongly enhanced mitochondrial fragmentation after application of oxidative stress. Thus, the increased sensitivity against oxidative stress in cells without functional PINK1 is possibly a consequence of an inability to phosphorylate and thus to activate the chaperone TRAP1 (summarized in Fig. 7). These findings correlate well with data demonstrating that a reduction of functional PINK1 protein increased the sensitivity of mouse brain and neurons against stress (Gautier et al., 2008; Haque et al., 2008).

Taken together, decreased Drp1 and Fis1 levels induced an elongation of mitochondria as well as a moderate elevation of PINK1 levels, and both features synergistically protect mitochondria of old cells against oxidative stress. However, in cases as the PD variant PARK6, stress would induce more severe mitochondrial fragmentation and oxidative damage, because of the lack of functional PINK1. This theory correlates with the progressive mitochondrial dysfunction in PD patients and is consistent with the age-related course of PD. Furthermore, reduced PINK1 expression in endothelial cells in vivo could also contribute to the age-related progression of arteriosclerosis, projecting an essential function of the ubiquitously expressed kinase PINK1 beyond its role in neurodegeneration.

Materials and Methods

Cell culture

HUVECs were purchased from Promocell (#C-12200) and cells were cultivated in endothelial cell growth medium (Promocell C-22010). Growth curves and doubling time were achieved from daily cell counts. To exclude the influence of genetic factors, HUVECs from at least three different isolations were used. The senescent status of HUVEC populations was verified by senescence-activated β-galactosidase staining (Dimri et al., 1995) with the senescence cells histochemical staining kit (Sigma) according to the manufacturer's instructions.

Constructs and transfection

Mt-PaGFP was previously constructed by Richard Youle (Karbowski et al., 2004). The ORF of Drp1 and Drp1K38A were cloned by Alexander van der Bliek (Smirnova et al., 1998). For the construction of GFP-Drp1 the original construct was digested with *Eco*RI and *Bam*HI and cloned into the *Eco*RI and *Bgl*II sites of the vector pEGFP-C1 (Clontech). Drp1K38A was made by Alexander van der Bliek (Smirnova et al., 1998). To obtain GFP-Drp1K38A, the ORF was amplified by PCR and cloned into the *Eco*RI and *Hin*dIII sites vector pEGFP-C1 (Clontech). GFP-Fis1 was constructed by amplifying the ORF of human Fis1 from cDNA of HUVECs as template and cloning into the *Bgl*II and *Eco*RI sites of vector pEGFP-C1 (Clontech). The plasmid PINK1-GFP 1 was constructed in the following way: a plasmid containing the human PINK1 in the vector pcDNA3.1 was obtained by Motoko Unoki and Yusuke Nakamura (University of Tokyo, Tokyo, Japan). The ORF of PINK1 was cloned into the *Nhe*I and *Hin*dIII sites of pEGFP-N1 (Clontech) after removing the stop codon. The point mutation G309D, which results in a mutated kinase domain, was introduced into plasmid PINK1-GFP 1 by directed PCR-mediated site-directed mutagenesis. For the plasmid PINK1-GFP2, the PINK1 ORF was amplified from HUVEC cDNA and cloned into the *Bgl*II and *Eco*RI sites of the vector pEGFP-N1 (Clontech). To obtain the plasmid SV40-PINK-GFP 2, the CMV promoter in front of the gene was deleted by digesting the plasmid with *Ase*I and *Bgl*II. The SV40 promotor sequence was amplified from plasmid pEGFP-N1 and cloned into the *Ase*I and *Bgl*II sites.

To achieve a transient knockdown of PINK1, the PINK1 antisense RNA HS_PINK1_4_HP_Validated siRNA (Qiagen) was used; for Fis1 knockdown, the Hs_Fis1_1 (Qiagen) and for Drp1 knockdown, the Hs_DNM1L_10 (Qiagen) was used. Allstars Negative Control siRNA (Qiagen) was used as a non-silencing control. 2 μg antisense RNA or plasmid DNA were transfected by electroporation using the HUVEC transfection kit (Amaxa) and nucleofector II (Amaxa). Stably expressing mt-PaGFP HUVECs were selected with G418 (250 μg/ml).

Irradiation

HUVECs were stained with MitoTracker Red CMX ROS (MTR) (Molecular Probes) and irradiated with light emitted from a mercury arc lamp (HBO 100). The light had to pass a filter that allowed only the passage of green light resulting in the excitation of the red dye MTR. The intensity was 0.3 J/cm^2 and irradiation time was 15 minutes unless indicated otherwise. To scavenge ROS, cells were first stained with MTR and after 1 hour, NAC (Sigma; final concentration 10 nM) was added to the cells 24 hours before irradiation.

Confocal laser-scanning microscopy

Mitochondrial membrane potential was determined by staining cells for 1 hour with dimethylaminostyrylmethyl-pyridiniumiodine (DASPMI) (gift from Bayer AG), at a final concentration of 2.5 μM. Micrographs were taken with a Leica SP5 confocal laser-scanning microscope fitted with the appropriate filters and a 63 (plan apochromat, 1.4 NA) objective that was controlled by the SCAN Ware 5.10 software (Leica). The images shown are representative of at least three independent transfections.

Quantification of mitochondrial morphology

MTR-stained irradiated and non-irradiated cells were fixed with 4% paraformaldehyde and examined at the indicated time points after irradiation (inverted microscope IM70, Carl Zeiss, Jena) equipped with a CCD camera (Sensicam, Till Photonics). At least 100 cells per sample were analyzed and the mitochondrial morphology was categorized into the morphotypes tubular, intermediate and fragmented.

Quantification of ROS

ROS were quantified by DHE staining intensity (Molecular Probes; final concentration 5 μM) after a 20 minute exposure to DHE. Pictures of the fluorescent samples were taken with constant microscope and camera settings. Micrographs were analyzed using ImageJ by calculating the integrated fluorescence of the oxidized ethidium in the nucleus only.

RNA isolation and semiquantitative RT-PCR

Methods for RNA isolation and semiquantitative RT-PCR for fission and fusion factors have been described (Jendrach et al., 2008).

RNA isolation, cDNA synthesis and qPCR

Whole RNA was isolated with the RNeasy mini kit (Qiagen) following the manufacturers instructions. For cDNA synthesis, 1 μg of total RNA was treated with DNase I (Invitrogen) and first strand synthesis was performed using the SuperScript III reverse transcriptase, oligo(dT)$_{20}$ and random primers (Invitrogen). qPCR was carried out using 30 ng cDNA per sample in a 20 μl reaction volume. For transcript detection, qPCR was performed using the StepOnePlus Realtime PCR System. To analyze transcript levels, the following TaqMan gene expression assays (Applied Biosystems) were used: PINK1, Hs00260868_m1; DNM1L, Hs00247147_m1; FIS1,

Hs00211420_m1; MFN1, Hs00966851_m1; MFN2, Hs00208382_m1; OPA1, Hs01047019_m1; MTP18, Hs00212905_m1; SLP2, Hs00203730_m1. TATA box binding protein (Tbp) (Hs99999910_m1), was used to normalize transcripts as a housekeeping gene. Changes in expression level were analyzed by using the $2^{-\Delta\Delta Ct}$ method.

Transcriptomics

SuperTAG-digital gene expression (ST-DGE) analysis was performed by GenXPro (Frankfurt/Main, Germany). ST-DGE is the adaptation of SuperSAGE, as described (Matsumura et al., 2006) to high-throughput sequencing using a Genome Analyzer Machine (Illumina, www.illumina.com). Tags were counted using the GenXProgram software and the likelihood of differential expression of each 26 bp tag was calculated using normalized tag numbers, with a correction for multiple tests (Audic and Claverie, 1997).

Western blotting

Proteins were separated by SDS-PAGE and then transferred onto a nitrocellulose membrane by semidry blotting. Fis1 was detected with an anti-Fis1 antibody (Sigma) and Drp1 with monoclonal anti-Drp1 antibody (BD Transduction laboratories). For detection of the bands, the NEB/BCIP system for detection of alkaline phosphatase activity was used. For analysis of total protein content. the actin levels were determined with a polyclonal anti-actin antibody (Sigma). The quantification of the respective grey values of all bands was achieved with the program ImageJ and the amount of Drp1 and Fis1 protein was normalized to the actin protein content. Oxyblotting has been described before (Strecker et al., 2009), and was performed with the OxyBlot Protein Oxidation Detection Kit (Millipore) following the manufacturer's instructions.

Statistics

Results are expressed as means ± s.e.m. of *n* experiments. ANOVA was used to compare sets of data and differences were considered statistically significant when $P<0.05$.

We thank Thomas Rudel (Berlin, Germany) for the DNA of the plasmids Drp1 and Drp1 K38A, Regina Voglauer (Vienna, Austria) for helping to generate stable transfected HUVECs and Karin Busch (Osnabrück, Germany) for plasmid mt-PaGFP. S.M. received a stipend from the Center of Membrane Proteomics (CMP), which is gratefully acknowledged. We also acknowledge support from the DFG (grant BE423/23-2), the EU (Integrated Project MiMage CT 2004-512020), the BMBF (NGFNplus NeuroNet Parkinson and GeronotoMitosys 0315584A) and the Parkinson Initiative of the University Frankfurt Medical School.

Supplementary material available online at
http://jcs.biologists.org/cgi/content/full/123/6/917/DC1

References

Audic, S. and Claverie, J. M. (1997). The significance of digital gene expression profiles. *Genome Res.* **7**, 986-995.

Bereiter-Hahn, J., Vöth, M., Mai, S. and Jendrach, M. (2008). Structural implications of mitochondrial dynamics. *Biotechnol. J.* **3**, 765-780.

Bossy-Wetzel, E., Barsoum, M. J., Godzik, A., Schwarzenbacher, R. and Lipton, S. A. (2003). Mitochondrial fission in apoptosis, neurodegeneration and aging. *Curr. Opin. Cell Biol.* **15**, 706-716.

Busch, K., Bereiter-Hahn, J., Wittig, I., Schägger, H. and Jendrach, M. (2006). Mitochondrial dynamics generate equal distribution but patchwork localisation of respiratory complex I. *Mol. Membr. Biol.* **23**, 509-520.

Chen, H., Detmer, S. A., Ewald, A. J., Griffin, E. E., Fraser, S. E. and Chan, D. C. (2003). Mitofusins Mfn1 and Mfn2 coordinately regulate mitochondrial fusion and are essential for embryonic development. *J. Cell Biol.* **160**, 189-200.

Collins, T. J., Berridge, M. J., Lipp, P. and Bootman, M. D. (2002). Mitochondria are morphologically and functionally heterogeneous within cells. *EMBO J.* **21**, 1616-1627.

Dimri, G. P., Lee, X., Basile, G., Acosta, M., Scott, G., Roskelley, C., Medrano, E. E., Linskens, M., Rubelj, I. and Pereira-Smith, O. (1995). A biomarker that identifies senescent human cells in culture and in aging skin in vivo *Proc. Natl. Acad. Sci USA* **92**, 9363-9367.

Erusalimsky, J. D. and Kurz, D. J. (2006). Endothelial cell senescence. *Handb. Exp. Pharmacol.* **176**, 213-248.

Exner, N., Treske, B., Paquet, D., Holmström, K., Schiesling, C., Gispert, S., Carballo-Carbajal, I., Berg, D., Hoepken, H. H., Gasser, T. et al. (2007). Loss-of-function of human PINK1 results in mitochondrial pathology and can be rescued by parkin. *J. Neurosci.* **27**, 12413-12418.

Frank S., Gaume B., Bergmann-Leitner E. S., Leitner W. W., Robert E. G., Catez F., Smith, C. L. and Youle, R. J. (2001). The role of dynamin-related protein 1, a mediator of mitochondrial fission, in apoptosis. *Dev. Cell* **1**, 515-525.

Gautier, C. A., Kitada, T. and Shen, J. (2008). Loss of PINK1 causes mitochondrial functional defects and increased sensitivity to oxidative stress. *Proc. Natl. Acad. Sci. USA* **105**, 11364-11369.

Gispert, S., Ricciardi, F., Kurz, A., Azizov, M., Hoepken, H. H., Becker, D., Voos, W., Leuner, K., Müller, W. E., Kudin, A. P. et al. (2009). PINK1-deficient mice show reduced movement activity and striatal dopamine, as well as progressive mitochondrial dysfunction. *PloS ONE* **4**, e5777.

Haque, M. E., Thomas, K. J., D'Souza, C., Callaghan, S., Kitada, T., Slack, R. S., Fraser, P., Cookson, M. R., Tandon, A. and Park, D. S. (2008). Cytoplasmic Pink1 activity protects neurons from dopaminergic neurotoxin MPTP. *Proc. Natl. Acad. Sci. USA* **105**, 1716-1721.

Hua, G., Zhang, Q. and Fan, Z. (2007). Heat shock protein 75 (TRAP1) antagonizes reactive oxygen species generation and protects cells from granzyme M-mediated apoptosis. *J. Biol. Chem.* **282**, 20553-20560.

Ishihara, N., Jofuku, A., Eura, Y. and Mihara, K. (2003). Regulation of mitochondrial morphology by membrane potential, and DRP1-dependent division and FZO1-dependent fusion reaction in mammalian cells. *Biochem. Biophys. Res. Commun.* **301**, 891-898.

Jahani-Asl, A., Cheung, E. C., Neuspiel, M., MacLaurin, J. G., Fortin, A., Park, D. S., McBride, H. M. and Slack, R. S. (2007). Mitofusin 2 protects cerebellar granule neurons against injury-induced cell death. *J. Biol. Chem.* **282**, 23788-23798.

James, D. I., Parone, P. A., Mattenberger, Y. and Martinou, J. C. (2003). hFis1, a novel component of the mammalian mitochondrial fission machinery. *J. Biol. Chem.* **278**, 36373-36379.

Jendrach, M, Pohl, S., Voth, M., Kowald, A., Hammerstein, P. and Bereiter-Hahn, J. (2005). Morpho-dynamic changes of mitochondria during aging of human endothelial cells. *Mech. Aging Dev.* **126**, 813-821.

Jendrach, M., Mai, S., Pohl, S., Vöth, M. and Bereiter-Hahn, J. (2008). Short- and long-term alterations of mitochondrial morphology, dynamics and mtDNA after transient oxidative stress. *Mitochondrion* **8**, 293-304.

Karbowski, M., Arnoult, D., Chen, H., Chan, D. C., Smith, C. L. and Youle, R. J. (2004). Quantitation of mitochondrial dynamics by photolabeling of individual organelles shows that mitochondrial fusion is blocked during the Bax activation phase of apoptosis. *J. Cell Biol.* **164**, 493-499.

Knott, A. B. and Bossy-Wetzel, E. (2008). Impairing the mitochondrial fission and fusion balance: a new mechanism of neurodegeneration. *Ann. N. Y. Acad. Sci.* **1147**, 283-292.

Kowald, A., Jendrach, M., Pohl, S., Bereiter-Hahn, J. and Hammerstein, P. (2005). On the relevance of mitochondrial fusions for the accumulation of mitochondrial deletion mutants: A modelling study. *Aging Cell* **4**, 273-283.

Lee, Y. J., Jeong, S. Y., Karbowski, M., Smith, C. L. and Youle, R. J. (2004). Roles of the mammalian mitochondrial fission and fusion mediators Fis1, Drp1, and Opa1 in apoptosis. *Mol. Biol. Cell* **15**, 5001-5011.

Lutz, A. K., Exner, N., Fett, M. E., Schlehe, J. S., Kloos, K., Lämmermann, K., Brunner, B., Kurz-Drexler, A., Vogel, F., Reichert, A. S. et al. (2009). Loss of parkin or PINK1 function increases Drp1-dependent mitochondrial fragmentation. *J. Biol. Chem.* **284**, 22938-22951.

Lyamzaev, K. G., Izyumov, D. S., Avetisyan, A. V., Yang, F., Pletjushkina, O. Y. and Chernyak, B. V. (2004). Inhibition of mitochondrial bioenergetics: the effects on structure of mitochondria in the cell and on apoptosis. *Acta Biochim. Pol.* **51**, 553-562.

Matsumura, H., Bin Nasir, K. H., Yoshida, K., Ito, A. and Kahl, G. (2006). SuperSAGE array: the direct use of 26-base-pair transcript tags in oligonucleotide arrays. *Nat. Methods* **3**, 469-474.

Nakada, K., Inoue, K., Ono, T., Isobe, K., Ogura, A., Goto, Y. I., Nonaka, I. and Hayashi, J. I. (2001). Inter-mitochondrial complementation: Mitochondria-specific system preventing mice from expression of disease phenotypes by mutant mtDNA. *Nat. Med.* **7**, 934-940.

Navratil, M., Terman, A. and Arriaga, E. A. (2008). Giant mitochondria do not fuse and exchange their contents with normal mitochondria. *Exp. Cell Res.* **314**, 164-172.

Neuspiel, M., Zunino, R., Gangaraju, S., Rippstein, P. and McBride, H. (2005). Activated mitofusin 2 signals mitochondrial fusion, interferes with Bax activation, and reduces susceptibility to radical induced depolarization. *J. Biol. Chem.* **280**, 25060-25070.

Ono, T., Isobe, K., Nakada, K. and Hayashi, J. I. (2001). Human cells are protected from mitochondrial dysfunction by complementation of DNA products in fused mitochondria. *Nat. Genet.* **28**, 272-275.

Perfettini, J. L., Roumier, T. and Kroemer, G. (2005). Mitochondrial fusion and fission in the control of apoptosis. *Trends Cell Biol.* **15**, 179-183.

Petit, A., Kawarai, T., Paitel, E., Sanjo, N., Maj, M., Scheid, M., Chen, F., Gu, Y., Hasegawa, H., Salehi-Rad, S. et al. (2005). Wild-type PINK1 prevents basal and induced neuronal apoptosis, a protective effect abrogated by Parkinson disease-related mutations. *J. Biol. Chem.* **280**, 34025-34032.

Poole, A. C., Thomas, R. E., Andrews, L. A., McBride, H. M., Whitworth, A. J. and Pallanck, L. J. (2008). The PINK1/Parkin pathway regulates mitochondrial morphology. *Proc. Natl. Acad. Sci. USA* **105**, 1638-1643.

Pridgeon, J. W., Olzmann, J. A., Chin, L. S. and Li, L. (2007). PINK1 protects against oxidative stress by phosphorylating mitochondrial chaperone TRAP1. *PLoS Biol.* **5**, e172.

Ramadass, R. and Bereiter-Hahn, J. (2008). How DASPMI reveals mitochondrial membrane potential: fluorescence decay kinetics and steady-state anisotropy in living cells. *Biophys. J.* **95**, 4068-4076.

Sandebring, A., Thomas, K. J., Beilina, A., van der Brug, M., Cleland, M. M., Ahmad, R., Miller, D. W., Zambrano, I., Cowburn, R. F., Behbahani, H. et al. (2009). Mitochondrial alterations in PINK1 deficient cells are influenced by calcineurin-dependent dephosphorylation of dynamin-related protein 1. *PLoS One* **4**, e5701.

Smirnova, E., Shurland, D. L., Ryazantsev, S. N. and van der Bliek, A. M. (1998). A human dynamin-related protein controls the distribution of mitochondria. *J. Cell Biol.* **143**, 351-358.

Stojanovski, D., Koutsopoulos, O. S., Okamoto, K. and Ryan, M. T. (2004). Levels of human Fis1 at the mitochondrial outer membrane regulate mitochondrial morphology. *J. Cell Sci.* **117**, 1201-1210.

Strecker, V., Mai, S., Muster, B., Beneke, S., Bürkle, A., Bereiter-Hahn, J. and Jendrach, M. (2009). Aging of different avian cultured cells: lack of ROS-induced damage and quality control mechanisms. *Mech. Ageing. Dev.* [Epub ahead of print].

Sugioka, R., Shimizu, S. and Tsujimoto, Y. (2004). Fzo1, a protein involved in mitochondrial fusion, inhibits apoptosis. *J. Biol. Chem.* **279**, 52726-52734.

Taguchi, N., Ishihara, N., Jofuku, A., Oka, T. and Mihara, K. (2007). Mitotic phosphorylation of dynamin-related GTPase Drp1 participates in mitochondrial fission. *J. Biol. Chem.* **282**, 11521-11529.

Tondera, D., Grandemange, S., Jourdain, A., Karbowski, M., Mattenberger, Y., Herzig, S., Da Cruz, S., Clerc, P., Raschke, I., Merkwirth, C. et al. (2009). SLP-2 is required for stress-induced mitochondrial hyperfusion. *EMBO J.* **28**, 1589-1600.

Unterluggauer, H., Hütter, E., Voglauer, R., Grillari, J., Vöth, M., Bereiter-Hahn, J., Jansen-Dürr, J. and Jendrach, M. (2007). Identification of cultivation-independent markers of human endothelial cell senescence in vitro. *Biogerontology* **8**, 383-397.

Valente, E. M., Abou-Sleiman, P. M., Caputo, V., Muqit, M. M., Harvey, K., Gispert, S., Ali, Z., Del Turco, D., Bentivoglio, A. R., Healy, D. G. et al. (2004). Hereditary early-onset Parkinson's disease caused by mutations in PINK1. *Science* **304**, 1158-1160.

Yang, Y., Ouyang, Y., Yang, L., Beal, M. F., McQuibban, A., Vogel, H. and Lu, B. (2008). Pink1 regulates mitochondrial dynamics through interaction with the fission/fusion machinery. *Proc. Natl. Acad. Sci. USA* **105**, 7070-7075.

Yoon, Y. S., Yoon, D. S., Lim, I. K., Yoon, S. H., Chung, H. Y., Rojo, M., Malka, F., Jou, M. J., Martinou, J. C. and Yoon, G. (2006). Formation of elongated giant mitochondria in DFO-induced cellular senescence: involvement of enhanced fusion process through modulation of Fis1. *J. Cell Physiol.* **209**, 468-480.

Zhou, C., Huang, Y., Shao, Y., May, J., Prou, D., Perier, C., Dauer, W., Schon, E. A. and Przedborski, S. (2008). The kinase domain of mitochondrial PINK1 faces the cytoplasm *Proc. Natl. Acad. Sci. USA* **105**, 12022-12027.

Zottini, M., Barizza, E., Bastianelli, F., Carimi, F. and Lo Schiavo, F. (2006). Growth and senescence of Medicago truncatula cultured cells are associated with characteristic mitochondrial morphology. *New Phytol.* **172**, 239-247.